

## Quenching Front Search Model of the SPACE Code

Seung Wook Lee\*, Sung Won Bae, Byung Jae Kim, Kyung Doo Kim  
Thermal-Hydraulic Safety Research Division, Korea Atomic Energy Research Institute, 111 Daedeok-Daero  
989beon-gil Yuseong-gu, Daejeon, Korea  
\*Corresponding author: nuclist@kaeri.re.kr

### 1. Introduction

A quenching front (QF) location plays an important role to determine the peak cladding temperature (PCT) and reflood quenching time during the reflood phase of a large break loss of coolant accident (LB-LOCA). Reflood during a LB-LOCA involves a very complicated two-phase and heat transfer phenomena in both pre-CHF and post-dryout conditions, i.e., droplet entrainment and quenching at the core region. Therefore, most of system analysis codes such as RELAP5 [1] and SPACE [2] have a capability of searching the QF location at the core region during a LB-LOCA. The existing QF searching logics of the SPACE code has been modified and the capability of the modified logics is demonstrated by comparing with existing one in this study.

### 2. Existing Quenching Front Search Model

Main parameters for the QF search model of the SPACE code are the critical heat flux temperature ( $T_{CHF}$ ) and minimum film boiling temperature ( $T_{MIN}$ ) which determine the wall heat mode and heat flux during a LOCA transient. Reflood quenching heat transfer model drastically increases the wall heat flux at the QF location and its effect decreases exponentially to 0.6 m higher than the QF [3]. Therefore, the QF location is a very important factor to determine the PCT in the reflood phase during LB-LOCA analysis. Note that the QF search model is not activated in the 1-D conduction model but 2-D conduction model.

#### 2.1 2-D Heat Conduction Model

The 2-D heat conduction model of the SPACE code can be activated by the user-specified trip event. For LB-LOCA analysis, this trip is usually activated during the reflood phase after the end of blowdown. Once the 2-D heat conduction model is activated, the axial heat flow as well as radial heat flow is calculated. A flow chart for the 2-D conduction model of the SPACE code is shown in Figure 1. As shown in the figure, the QF search model is called first after activation of 2-D conduction. Then fine node rezoning is performed to subdivide 2-D basic axial node into smaller node only if the 1-D node index containing the QF (qf\_1d) is available. If not, 2-D basic axial node is preserved without fine node rezoning.  $T_{CHF}$  and  $T_{MIN}$  are determined in the wall heat mode and heat transfer coefficient function, respectively as shown in the figure.

The index of qf\_1d is required for tracing the QF location correctly when the QF crosses at the point of interface of each 1-D node and it will move to the same direction (upward or downward) of the QF movement.

#### 2.2 Bottom Quenching Front Search Model

The existing QF search model seeks for the location of bottom QF only. A flow chart of the existing QF search model is shown in Figure 2. As shown in figure, the QF location is initialized to zero, and the search model begins to inquire out the QF location from the bottom of fuel rods. If the wall temperature ( $T_w$ ) at the current fine node is below  $T_{CHF}$  and the heat transfer mode condition is satisfied, the current fine node is assumed to be quenched and QF location is changed to the current node elevation. This search logic continues until either current node reaches the top of fuel or hot wall condition ( $T_w > T_{CHF}$ ) is satisfied, and as a result, the QF is determined whether it exists or not. If the QF location is not zero, the QF exists and qf\_1d can be also determined. If not, qf\_1d is not available because the QF doesn't exist.

### 3. Modified Quenching Front Search Model

A flow chart for the modified QF search model is shown in Figure 3. There are three main differences between the existing and the modified models:

- (1) The model for  $T_{CHF}$  is modified.
- (2) The minimum liquid fraction is added for the wetted wall condition.
- (3) A top QF search model is added.

The other model except for above three conditions, are not changed in the modified model.

$T_{CHF}$  used in the existing model is modified as follows:

$$T'_{CHF} = T_{CHF} + 0.2(T_{MIN} - T_{CHF})$$

$T_{CHF}$  of the modified model is higher than that of the existing model and as a result, the possibility of hot wall quenching is reduced compared with the existing model.

The restriction of the minimum liquid fraction is introduced to avoid earlier quenching when the liquid fraction is very low. Currently the setpoint of minimum liquid fraction is set to 0.05 at the bottom of the core and linearly increases by 0.1 at the top of the core. The liquid fraction of 0.05 is selected since it is the

boundary of interpolation region between single phase vapor convection and nucleate boiling heat transfer.

The top QF search model is newly introduced in the modified model. The basic logic searching for the top QF is almost the same as the bottom quenching model except that the initial QF location is not zero but total height of the core and the searching order is from top to bottom in the opposite direction to the bottom QF search. In addition, the setpoint of the minimum liquid fraction does not depend on the elevation, but is fixed to 0.05.

#### 4. Evaluation Test

In order to evaluate the modified QF search model, comparative simulations for ARP1400 LB-LOCA have been performed.

Figure 4 shows the comparison result of the bottom QF location for both existing and modified search model. As shown, there is no remarkable difference between two results. However, it is clear that the final bottom quenching location of the modified QF model is lower than that of the existing one because the top QF model has been applied in the modified QF model.

A comparison result for the top QF location is shown in Fig. 5. Apparently, the top QF of the modified model changes as the top quenching advances, but the top QF of the existing one doesn't change because of the absence of the top QF search model.

Figure 6 shows the temperature behavior of hottest core where the maximum PCT occurs. The quenching time is delayed slightly in the modified search model. This discrepancy results from the higher  $T_{CHF}$  and the restriction of the minimum liquid fraction in the modified model.

#### 5. Conclusions

For a more realistic simulation of reflood phase during LB-LOCA of APR1400, a modified quenching front search model has been implemented into the SPACE code. It has three different features compared with the existing QF model; i) The model for  $T_{CHF}$  is modified, ii) The minimum liquid fraction is added for the wetted wall condition, iii) A top QF search model is added. In order to evaluate the enhancement of new model, comparative simulations for ARP1400 LB-LOCA have been performed. As a result, delayed quenching time and top quenching phenomena have been observed as expected. Especially, the existing model never predicted top quenching phenomena. Because the analysis capability of the modified QF search model is better than to the existing one, new model is replaced with old one.

#### Acknowledgment

This work was supported by the Nuclear Power Technology Development Program of the Korea Institute of Energy Technology Evaluation and

Planning (KETEP) grant funded by the Korea Government Ministry of Knowledge Economy.

#### REFERENCES

- [1] RELAP5/MOD3.3 Code Manual, Volume I: Code Structure, System Models and Solution Methods, NUREG/CR-5535/Rev 1, INEEL, December (2001)
- [2] Ha, Sang Jun et al., Development of the Space Code for Nuclear Power Plants, Nuclear Engineering and Technology, p.45 ~ p.62, Vol.43, No.1, Feb. 2011.
- [3] S. K. Moon *et al.*, Design Report of the Wall Heat Transfer Correlation of the SPACE Code, S06NX08-A-1-RD-11, Rev. 2, KAERI, 2012. 12.

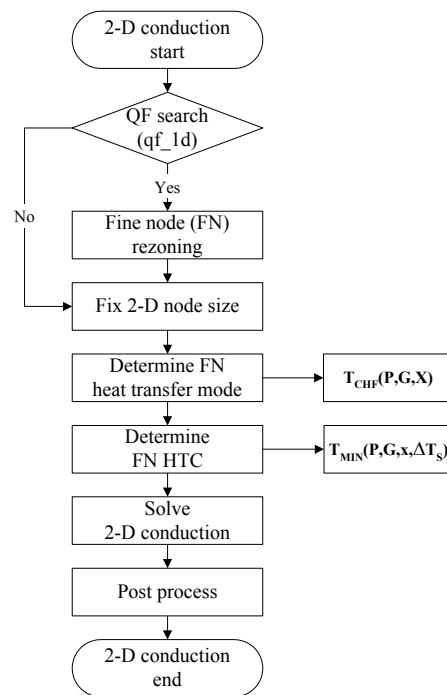


Fig. 1 Flow chart for 2-D conduction model

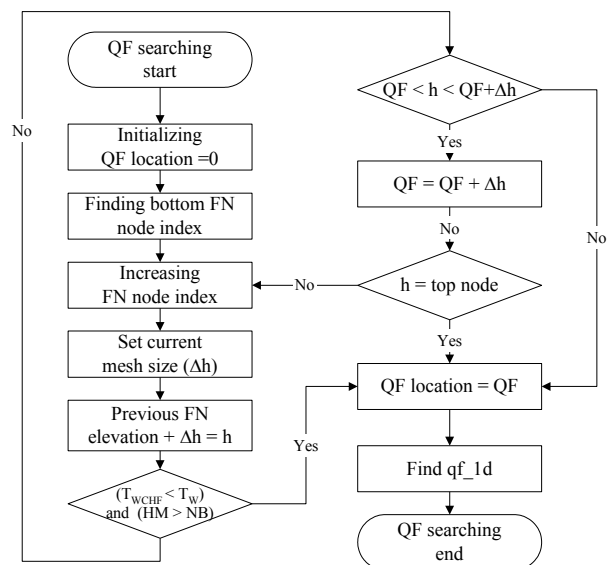


Fig. 2. Flow chart of existing bottom QF search model

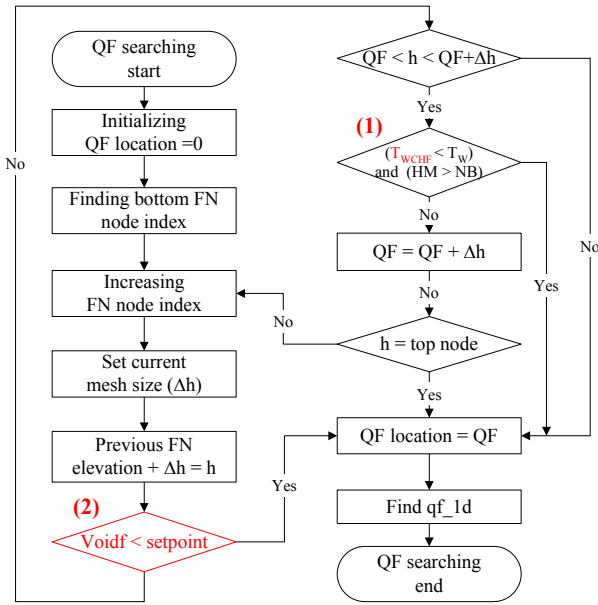


Fig. 3. Flow chart of modified bottom QF search model

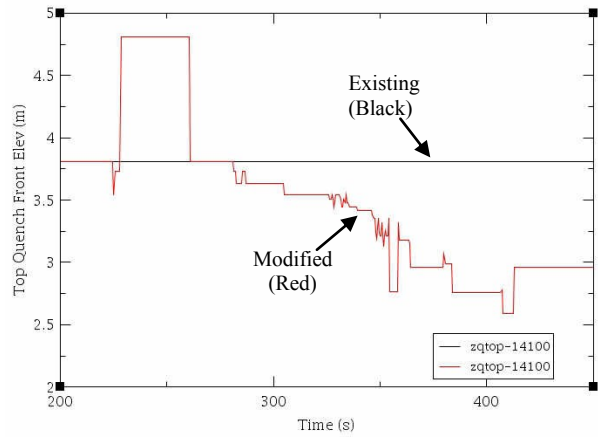


Fig. 5. Comparison of top QF location

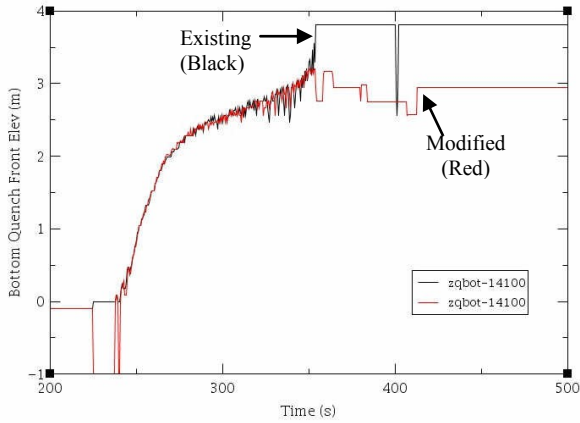


Fig. 4. Comparison of bottom QF location

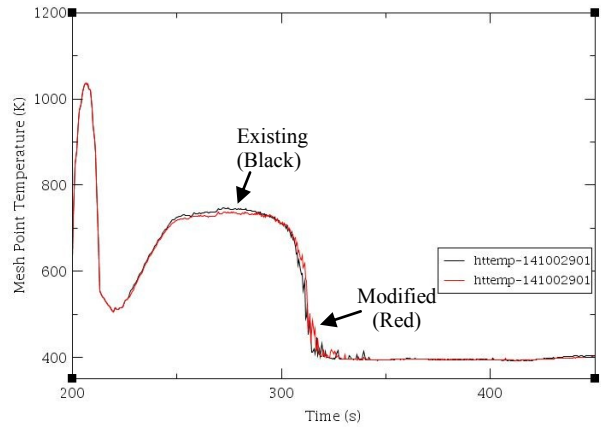


Fig. 6. Comparison of maximum PCT